OPTICAL METHODS FOR WATER POLLUTION MONITORING

MÉTODOS ÓPTICOS PARA MONITORIZAÇÃO DE POLUIÇÃO DA ÁGUA

Andrei B. Utkin, Alexander V. Lavrov, Rui Vilar, Sergey Babichenko, Sergey Shchemelyov, Innokenty Sobolev, Luísa Bastos, Richard A. Deurloo, Jesús Torres Palenzuela, Nina V. Yarovenko, Isabel Cruz

ABSTRACT

An innovative optical method for remote monitoring of water pollution was developed and tested in AMPERA ERA-NET Programme, project DEOSOM. The method is based on remote detection of laser-induced fluorescent radiation (LIF LIDAR). In the project, compact and light LIF LIDAR systems were developed, which can be operated by relatively unskilled personnel and used for early air- or shipborne pollution detection and evaluation, specifically for oil spill detection. The systems are provided with direct georeferencing, for exact localization of the oil spills, and artificial intelligence, for their automatic characterization. The paper presents the principles of the method and the results of tests carried out in the field and laboratory conditions.

Keywords: Laser Induced Fluorescence; Remote Detection; Pollution; Oil Spill.

RESUMO

Um inovador método óptico para a monitorização remota da poluição aquática foi desenvolvido e testado no âmbito do projecto DEOSOM financiado pelo programa AMPERA ERA-NET. O método é baseado na detecção remota de radiação fluorescente induzida por laser (LIF LIDAR). No projecto foram desenvolvidos detectores LIF LIDAR compactos que podem ser utilizados por pessoal sem qualificação específica para a detecção precoce e avaliação da poluição através de aeronaves e embarcações, especificamente na detecção de derrames de petróleo. Os sistemas são fornecidos com georreferenciação directa, para a localização exacta do derramamento, e inteligência artificial, para a sua caracterização automática. O artigo apresenta os princípios em que baseia o método bem como os resultados dos testes realizados em campo e em laboratório.

Palavras-chave: Fluorescência Induzida por Laser; Detecção Remota; Poluição; Derramamento de Petróleo.

JEL Classification: Q53

1. INTRODUCTION

Due to the increasing traffic of cargo ships and tankers in European waters, the risk of water pollution by accidental or criminal oil spillage is increasingly high. The same

situation occurs in the more than 1100 ports in the European Union. Ships and offshore installations are the most common sources of more than 500,000 tons of oil spilled into the marine environment every year.

Oil spillage monitoring includes three levels of surveillance. The first level is satellite-borne (range about 50 to 200 km); the second level consists of airborne inspection by visual analysis and IR/UV sensors (range about 100 to 500 m); the third level of surveillance is waterborne. For many years the attention of scientists and engineers was concentrated mainly on the development of detection methods and equipment for the first and second levels of surveillance. A number of active and passive optical methods were developed, mainly using complex and costly instruments. As a result, only very few detection methods are currently available for the 3rd level of surveillance, one of the most important, due to its flexibility and lower cost. In particular, the need for lightweight, low-cost detectors that can be widely used for watercraft borne as well as airborne coastal inspection remained unmet.

In response to this demand, in the end of 2008 a consortium of university, government and industry researchers listed in Table 1 launched a project aiming at developing an efficient system for shipborne pollution surveillance in harbourages, rivers, channels, and coastal waters. This three-year project, named DEOSOM (Detection and Evaluation of Oil Spills by Optical Methods) was funded within the European Coordination Action to Foster Prevention and Best Response to Accidental Marine Pollution (AMPERA, 2007). It had the following objectives:

1. Developing a low cost nanometre-spectral-range fluorescence LIDAR for early detection of oil spills in riverine and coastal waters and measurement of the hydrocarbon film thickness.
2. Developing a dedicated low-cost direct georeferencing system (GPS/GNSS+IMU) allowing for oil spillage mapping.
3. Benchmarking of the fluorescence lidar developed in the project against more sophisticated well established techniques.

Table 1: Consortium of the DEOSOM Project

Institution	Location	Principal role
INOV (INOV - INESC Inovação)	Lisbon, Portugal	Project coordination, general research and design, system integration
LDI (Laser Diagnostic Instruments AS)	Tallinn, Estonia	Development of optical detectors
CIIMAR (Centre of Marine and Environmental Research)	Porto, Portugal	Development of communication and positioning system
UVigo (University of Vigo)	Vigo, Spain	Planning and organisation of field tests and data processing
IH Instituto Hidrográfico	Lisbon, Portugal	Providing general methodology and conducting specific laboratory tests

The present paper reviews the main results achieved during the project execution and discusses these developments in a market prospective.

2. THIRD-LEVEL WATER-POLLUTION SURVEILLANCE: AN OPTICAL APPROACH

The methods presently available for the third-level water pollution surveillance usually rely on ultraviolet (UV), visible or infrared (IR) imaging. Scanners are predominantly used as sensors in the visible region of the spectrum. These systems can detect oil under optimum conditions, but the inherent lack of positive discrimination between oil and some backgrounds limits their applicability. In addition, thin oil films on the water surface are often invisible even in daylight and good weather conditions (Fingas and Brown, 2007).

Detectors based on laser-induced fluorescence (LIF) light detection and ranging (LIDAR) are far more useful instruments due to the capability of this method to reliably detect and, in appropriate conditions, identify oil against soil, water, ice and snow backgrounds. The principles of LIF LIDAR are illustrated in figure 1.

Figure 1: Principal sketch of a LIF LIDAR detector

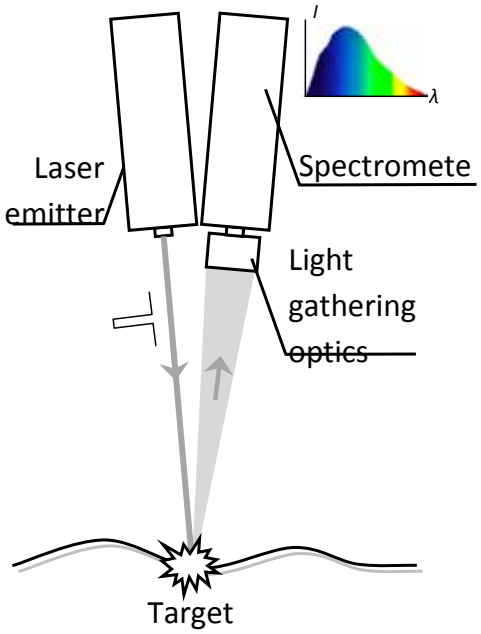

The radiation emitter, comprising a pulsed laser and beam-forming optics, produces short (~1 – 10 ns) and intense radiation pulses, which propagate through the atmosphere. When the emitted beam hits a target, the laser radiation interacts with the target's molecules, leading, for many chemical compounds, to the emission of radiation with longer wavelengths via fluorescence. A fraction of this radiation, propagating back to the detector, is collected by a telescope and directed to a spectrometer for spectral analysis. The spectra are recorded in digital form in a computerized data-acquisition unit. The angular position of the emitted laser beam and the detection time of the return radiation pulse allow calculating the position of the target, while the spectrum gives the target chemical composition.

As air- and shipborne LIF LIDARs change their positions during measurements, the signals are time stamped and georeferenced to allow calculating the absolute location of the target for each measurement and, thus, mapping the pollutant distribution.

Water pollution monitoring can also be implemented by pumping water into the detector and irradiating its internally with a flashlamp, providing the complementary opportunity to vary the excitation wavelength. This variation adds one more dimension to

fluorescence spectra, turning them into two-dimensional spectral fluorescence signatures (SFS) akin to one illustrated in figure 2.

The choice of the detector strongly depends on the application, especially on the area under surveillance as well as on the promptness and reliability of pollution detection and characterisation (fingerprinting).

Figure 2: An example of spectral fluorescence signature represented as surface (left) and contour (right) plots

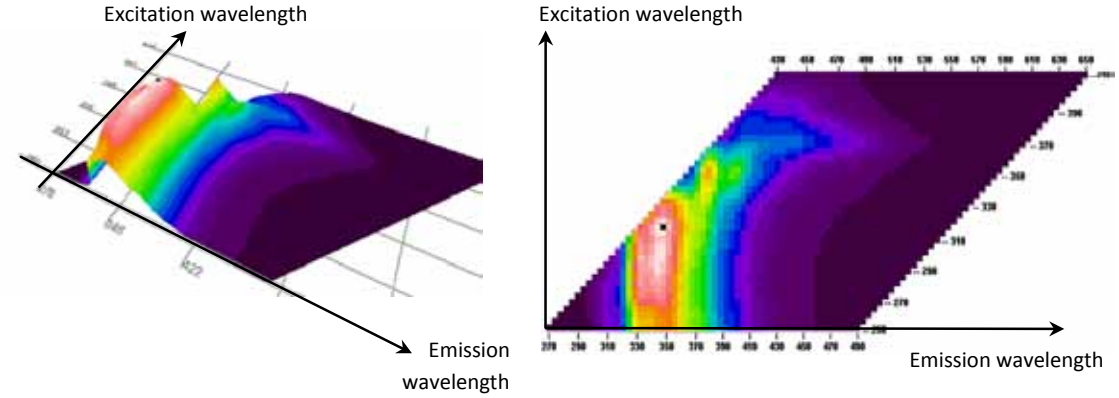

3. BASIC COMPONENTS OF LIF LIDAR WATER POLLUTION DETECTORS

3.1 Radiation sources

The laser used as radiation source defines the excitation-pulse energy and wavelength - parameters that determine the detection range and the set of detectable pollutants.

Excimer XeCl lasers provide ultraviolet radiation at 308 nm wavelength. The main advantage of this solution is a good spectral separation of the principal spectral signatures to be detected: the peak due to water Raman scattering appears in the range 340-345 nm, the maxima of the fluorescence response of oils are in the 400-450 nm region, and the dissolved organic matter (DOM) fluorescence appears in between (at 350-400 nm). In addition, the laser beam penetrates deeply in water, allowing to detect submerged oil. The disadvantages include high acquisition and maintenance costs and the necessity of a gas supply, which increases the complexity of the instrument and reduces the ease of transportation.

Nd:YAG lasers emitting in the fundamental wavelength (1064 nm) are not suitable for the application, but the frequency duplication and triplication yields 532 and 355 nm radiation in the visible and ultraviolet ranges respectively, sufficiently energetic for efficient excitation of hydrocarbon fluorescence. The second harmonic of the Nd:YAG laser is less convenient for LIF LIDAR measurements due to lower quantum yield and eye hazard. For the 355-nm excitation, the water Raman peak lies at ~400 nm, the maximum of DOM emission in the region from 400 to 500 nm, and the oil fluorescence between 420 and 650 nm, thus making the separation these two signatures a more difficult task (see figure 3). Water penetration for 355-nm radiation is lower than for 308 nm, so this laser is preferably used for surface detection. On the other hand, the acquisition and maintenance costs for such instruments are significantly less than for XeCl excimer LIF LIDARs, and these lasers do not require gas.

Figure 3: LIF spectrum of a thin Marlin crude oil film on the water surface (black) plotted together with LIF spectra of water, predominantly composed by DOM (red) and pure Marlin oil (green). The oil film spectrum corresponds well to a combination of the DOM and oil spectra (dotted blue) taken, respectively, with the coefficients 1.01 and 1.001, found via the least mean squares method.

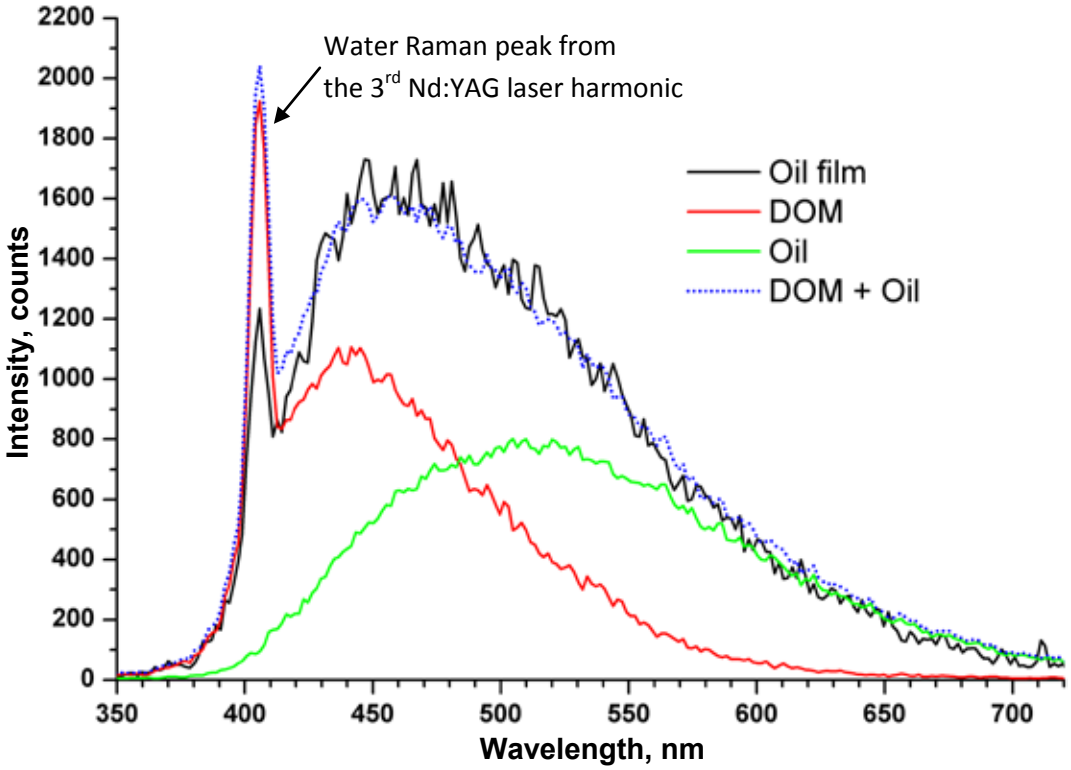

Recent developments in the optoelectronic industry brought the opportunity of constructing LIF LIDAR detectors on the basis of UV diode lasers. Producing weaker light and having far worse beam quality than Nd:YAG lasers, diode lasers are adequate for short-range detection. However, their low price, weight, dimensions and energy consumption, as well as long durability and minimum servicing requirements make these lasers extremely attractive for water-borne pollution monitoring. Of particular importance is their potential for autonomous operation using, for example, solar powering. By using one of these lasers and low-weight optical design, a LIF LIDAR instrument available for buoy-based maritime surveillance could be built.

3.2 Light gathering optics

The light gathering optics collects the radiation emitted from the target and focuses it in the entrance slit of the spectrometer. The radiation is usually collected by a telescope, and the power of the detected radiation is proportional to the area of its input pupil defined by the first lens. The choice of this lens diameter is a trade-off between sensitivity and compactness/weight.

Gathered radiation is usually transported to the spectrometer by optical fibre. In this case it is the fibre core that constrains the input aperture of the spectrometer, thus making unnecessary introduction of the optical slit unit. However, the schemes comprising a telescope rigidly connected with the spectrometer through an optical slit unit provide more efficient radiation conversion and an additional opportunity of establishing an ad

hoc trade-off between the spectral resolution and sensitivity though adjustment of the slit width.

In general, an optical filter is introduced in the light pass to protect the spectrometer from retroreflected excitation radiation.

3.3 Spectrometers

As oil fluorescence emission spreads over a wide spectral range, the fluorescence oil-spill monitoring requires broadband spectral detectors. A great variety of detectors have been employed in the LIF LIDAR technique, including optical multichannel analyzers, photodiode array detectors, and nonintensified and intensified charge coupled devices, usually referred to as CCDs and ICCDs. The choice of the detector depends on many factors, including data acquisition rates and type of signal processing, sensitivity, spectral range, field deployability, and overall system cost (Carranza et al., 2003).

For portable low-cost instruments, palm-size Czerny-Turner CCD spectrometers price (figure 4) are often used.

Figure 4: Czerny-Turner optical bench: a basis for compact mass-production CCD spectrometers

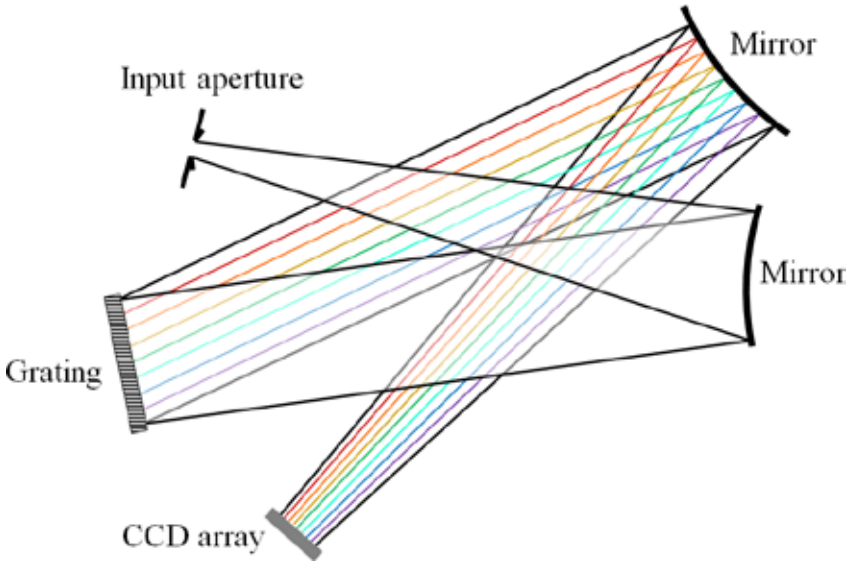

The ICCD spectrometers — despite of the higher cost, as compared to their CCD counterparts — provide much better sensitivity, with improvements in SNR ranging from a factor of 3 to greater than 1 order of magnitude (Carranza et al., 2003). This is especially important for long-range applications, such as the airborne surveillance, and for systems employing low-power sources.

In the LIF LIDAR technology, the contemporary global tendency of optimisation via integration is embodied in combining light gathering and spectral decomposition within the framework of a unique receiver system with lesser number of elements. An example of such a system, in which the diffraction grating plays an additional role of an imaging mirror is given in figure 5.

Figure 5: ICCD receiver with an adjustable telescope from Laser Diagnostic Instruments in which the diffraction grating plays an additional role of an imaging mirror (LDI, 2010)

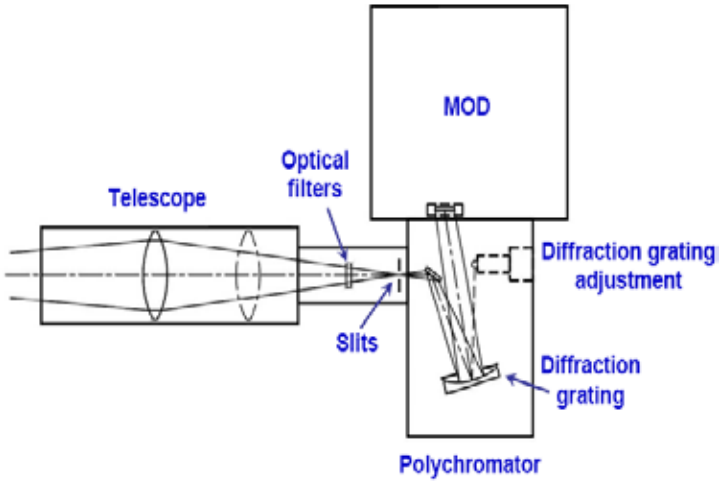

3.4 Georeferencing

There are many global navigation satellite systems (GNSS) available in the market, from simple code navigation equipment to single or double frequency phase receivers, which range significantly in accuracy and price, operating in either the precise point positioning (PPP) or differential mode.

Totally autonomous inertial georeferencing system may be used as an alternative or as a complementary sensor. The inertial systems are categorised according to the type of their principal element, a gyroscope. Three types of gyroscopes are in wide use: MEMS (Micro-Electro-Mechanical Systems), fibre-optic (FOG), and ring-laser (RLG) ones. The MEMS are typically considered low cost gyroscopes, while FOG and RLG sensors represent medium to high cost systems. Some last-generation MEMS can compete with FOG systems, although the latter still have superior temperature stability.

Through the integration of GNSS measurements with inertial data the weaknesses of each system can be overcome. GNSS can be used to control the drift in the IMU solution and the IMU data can be used to bridge the gaps when there is loss of lock of the GNSS signal.

The final solution is the precise position and orientation of a moving platform/sensor at each instant.

3.5 Control software

The top layer software controls data acquisition process and merges the spectra with the time stamp, necessary for synchronisation with the georeferencing data. The control involves a series of operations, such as the laser-beam positioning, initiating the laser pulse, background measurements, etc., and thus the control system is responsible for simultaneous operation of numerous peripheral devices, prompt error handling and providing a graphical user interface (GUI). Although Windows is not a real-time operating system (OS), it suits the present application because when the low pulse frequency lasers (~10 Hz and less) are used, the intra-pulse time is sufficiently long for the OS to finish the critical operations by the time of the next measurement.

The components can be controlled directly by the computer through the memory-mapped (MMIO) and/or port-mapped (PMIO) input/output (McDougall and McDougall, 2011). Such an approach used to be cost-effective as it does not require any extra processing

devices. However, with the widespread of cheap integrated circuits, today's dominating tendency is to provide the real-time data processing with the help of a microcontroller built-in in the data acquisition circuit, see, for example, (Ocean Optics, 2011) and a flow chart of figure 6. The most challenging task in developing such combined packages is to provide the reliable connectivity and simultaneous work of the built-in controller and PC software.

Figure 6: LDI detector for water- and airborne LIF LIDAR applications: schematics of the control (Alekseyev et al., 2008)

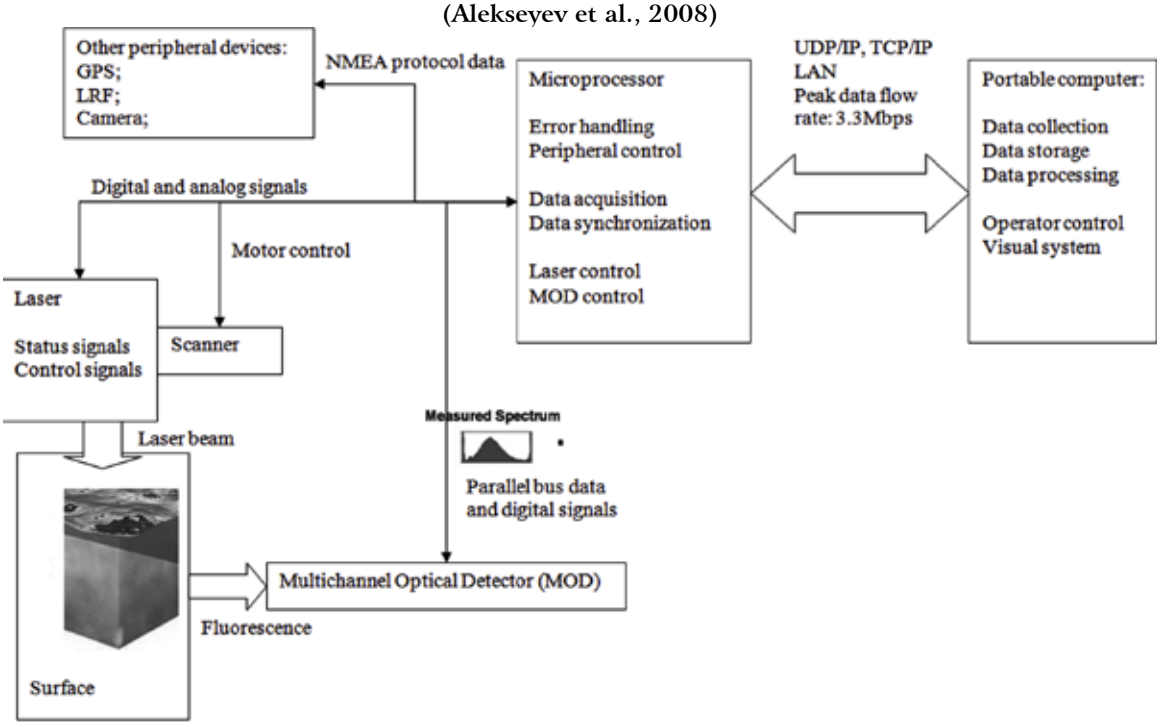

4. DEVELOPED LIF LIDAR DETECTORS

The LIF LIDAR detectors developed during the project include sufficiently wide range of instruments, differing in detection capabilities and prices. The most expensive instrument shown in figure 7, equally suited for water- and airborne applications, has the detection range of several hundred meters and possibility to detect submerged spills of hydrocarbon pollutants.

Figure 7: Compact LIF LIDAR detector based on a XeCl laser (excitation wavelength is 308 nm). The detector has dimensions of 60×50×40 cm^3, isolated and waterproof case, and waterproof LAN and electrical connections

Similar LIF LIDAR instruments developed on the basis of frequency-doubled and tripled Nd:YAG laser is shown in figure 8. Producing the excitation radiation at the wavelengths of 532 and 355 nm correspondingly, this detector is unable to detect submerged oil spills, and here the separation of DOM and oil signatures is more challenging than in the case of shorter-wavelength 308 nm excitation. However, such a scheme may result in more compact and cheaper instruments.

Figure 8: LIF LIDAR detector prototype based on a Nd:YAG laser, producing the excitation radiation at 355 and 532 nm: operation during the field tests in Vigo (Utkin et al., 2011)

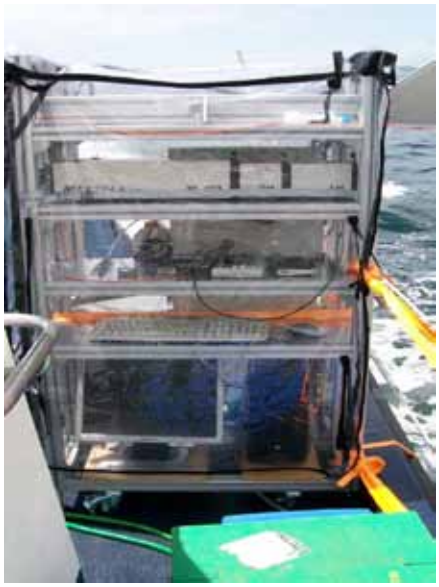

The chipset LIF LIDAR detector design is based on the cost-effective UV laser diodes (figure 9). The weak signal of fluorescence excited by low-energy laser diode is detected in a few number of wide spectral bands, resulting in sufficiently rough characterisation of the spectrum, but enabling the detection range to stay within acceptable limits of tens to hundred meters, depending on the pollutant type.

Figure 9: LIF LIDAR detector prototype based on a UV diode laser (Babichenko and Shchemelyov, 2011)

5. SIGNAL PROCESSING AND SPECTRUM CHARACTERIZATION

LIF signal processing includes the background elimination and accumulation of spectra from several laser pulses. In most cases the background elimination is performed by low-level microprocessor software, which, being switched into the pulse-synchronisation mode, forces the spectrometer to measure three spectra instead of one. The measurements are taken before, simultaneously with, and after the laser pulse, and the average of the first and third spectra is taken as the background level, to be subtracted from the main second measurement. The background spectra hold different constituents of noise like sun flares, temperature and electronic noise can be excluded from the LIF spectrum by subtraction.

Oil fluoresces mostly due to its aromatic compound components and thus is strongly influenced by the chemical composition and physical characteristics (e.g., viscosity and radiation extinction coefficient) of the oil (Ryder, 2005).

The laser induced spectrum of oil films on water contains components not related to oil fluorescence, namely the water Raman scattering and LIF emission from dissolved organic matter (DOM). The Raman scattering peak of oil-contaminated water is attenuated by absorption of both the excitation and scattered radiation in the hydrocarbon film, so the attenuation factor can be used to estimate the oil-film thickness. DOM fluorescence complicates the spectral analysis and may prevent oil identification. On the other hand, the DOM signal can carry important information on the organic contamination of water. Since the intensity of water Raman scattering is an indicator of water transparency, the LIF intensities can be normalized by the Raman intensity to provide an absolute scale of the oil and DOM pollution emission.

Oil fingerprinting on the basis of the LIF spectra must be based on fast algorithms, which enable the user to change the vehicle trajectory in real time, in accordance with the current detection results. As a rule, such algorithms utilize reduction of information via feature extraction and perform a two stage analysis: (1) pollution detection and (2) identification of the pollutant(s).

An example of feature extraction for pollution detection is given in figure 10. The integral spectral intensities R, A, and B within the marked spectral ranges for a clean water spectrum (figure 10a) serve as a reference. The first range is defined by the inflections of the spectrum due to the water Raman peak (wavelengths λ_1 and λ_2), and the value of R is calculated as an integral of the spectral intensity above the line passing through the deflection points. The second spectral range starts at λ_2 and extends to the DOM fluorescence maximum λ_3, and the integral intensity A is calculated by integration above the background line defined by the spectral intensities at λ_2, λ_3. The (λ_2, λ_3) range is further split into two equal width sub-ranges (by the red dashed line in figures 10b, c), yielding the integral intensities A_1 and A_2. The case $A_1 > 0$ and $A_2 > A$ (figure 10b) corresponds to polluted water and that of $A_1 < 0, A_2 > A$ (figure 10c) indicates heavily polluted water. The value of B (figure 10a) can be applied to detect changes in DOM composition in the area of observation on condition that $A_2 = A$. An increase of the current value of B as compared to that of clean water often indicates a higher ratio of terrestrial DOM fractions, typically testifying a shore discharge (Babichenko et al., 2006).

Figure 10: Feature extraction for pollution detection based on spectral shape variation (Babichenko et al., 2006)

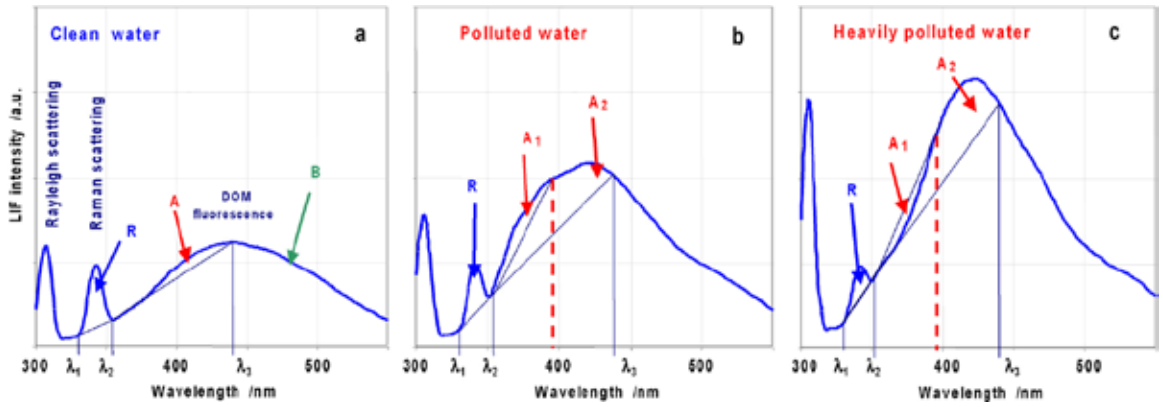

Identification of the pollutant oil is a more challenging task as one cannot predict a certain spectral signature or feature from the petroleum nomenclature based on empirical macroscopic properties (gravity, viscosity, etc.). It is therefore necessary to investigate the optical properties of a representative number of different oil types in the laboratory, and to analyze the spectral variability of their signatures. Obviously, it is impossible to investigate the optical properties of all different oils transported at sea. This has to be done with a number of representative oils, whereby the term "representative" does not necessarily have a global meaning. In most cases local or operational aspects should also be taken into consideration.

One of the earliest oil recognition method was proposed by Hengstermann and Reuter (1992). It is based on the principal component analysis. The eigenanalisys of the covariance matrix of 51 spectra of a representative catalogue of crude oils and refined products has shown that only four first basic spectral forms (eigenspectra) contain 99% of the information of the catalogue.

Another approach to oil detection and classification is based on the artificial-intelligence algorithms implemented via distributed systems with variable parameters, adjustable during a supervised leaning procedure. One classification system developed within the DEOSOM project (Martín et al., 2011; Torres et al., 2011), is schematically represented in figure 11. The subsystem dedicated to pollution detection is based on a one-class support vector machine (OC SVM). It classifies the spectra into two classes, representing unpolluted water and water with some anomalous LIF emission. By means of OC SVM a classification model is trained using only unpolluted water data, and each new sample not fitting the unpolluted water spectrum is considered to be an anomaly.

Figure 11: Pollution detection and identification algorithm developed within the framework of the DEOSOM project (Torres et al., 2011)

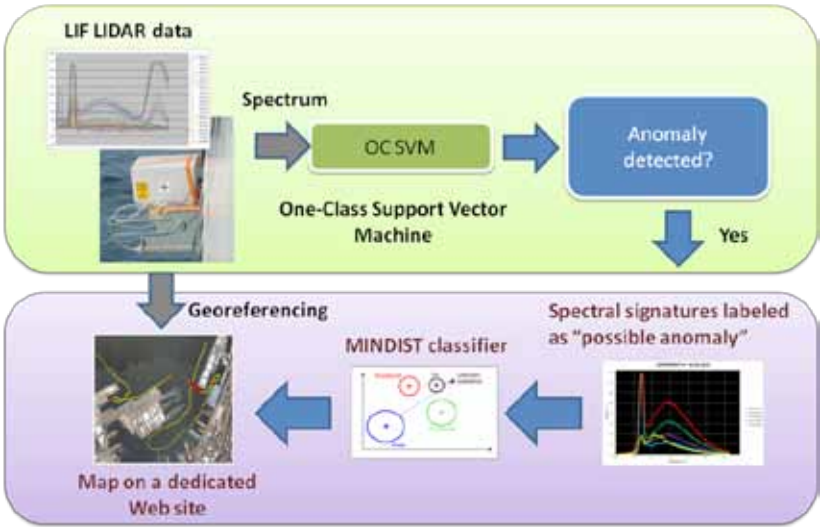

The subsystem dedicated to the pollutant identification is based on oil signature recognition. After analysis of the spectral signature variability of pertinent hydrocarbons, a database composed of 12 distinct oil products transported through and processed in Galicia was built. The LIF spectrum of each product is represented by a 512-points (wavelengths) reference vector. Anomalous LIF emission is also represented by a vector of the same dimension. The classification of these vectors is performed by comparing their Euclidian distances in the 512-dimensional space to each of the reference vectors. The signature is attributed to the oil product corresponding to the nearest reference vector (minimum distance, so-called MINDIST algorithm). The processing chain of the classifier contains a web server interface based on open source technologies: Google Earth engine, Open Layers java script and Map Server. The onboard software interacts with the server (additionally providing the georeferencing data) and receives the classification results promptly inserted into the electronic map of the locality.

Other important direction in the development of oil-recognition algorithms is developing software for subdivision of oils into common classes, like light, heavy and extra heavy, on the basis of their LIF emission. Since this classification is usually done on the basis of physicochemical parameters, such as the aromatic composition and specific, the correlation between these two parameters and specific features that can be extracted from the LIF spectra must be analyzed. The scattergraphs of the relative populations of hydrocarbon molecules containing only one aromatic ring I_1 and five or more aromatic rings $I_{\geq 5}$ (%) versus the relative LIF spectrum maximum F_m for eight chosen crude oil brands (Agbami, Asgard, Azeri Light, Brega, Marlin, Mellitah, Sahara Blend and Zafiro Blend) are shown in figure 12. The aromatic composition of the oil samples was assessed on the basis of laboratory fluorometric experiments carried out by Instituto Hidrográfico (Lisbon) using the methodology developed by Law (1980).

Figure 12: Scattergraphs of the relative aromatic-ring populations I_1 and $I_{\geq 5}$ (%) versus the relative LIF spectrum maximum F_m

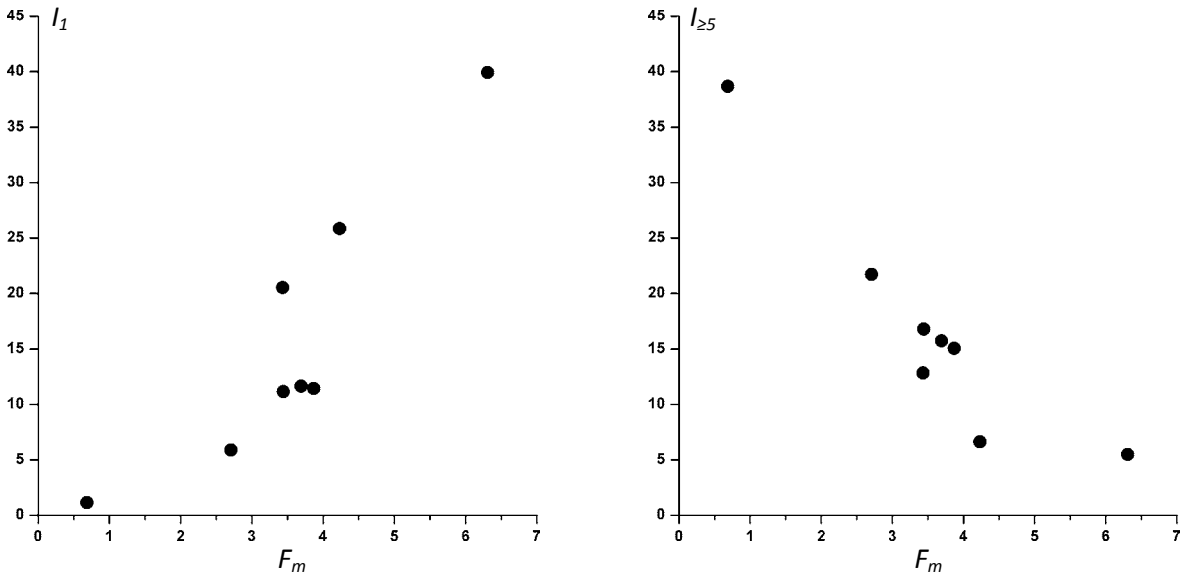

The figure indicates strong correlation between the parameters under comparison; the quantitative results for the whole set of populations assessable with Law's method, $\{I_1, I_2, I_{34}, I_{>5}\}$, are presented in Table 2.

Table 2: Correlation coefficients between the relative aromatic-ring populations $\{I_1, I_2, I_{34}, I_{\geq 5}\}$ and the relative LIF spectrum maximum F_m

Aromatic-ring population	Correlation coefficient
I_1 (one aromatic ring)	0.90
I_2 (two aromatic rings)	0.71
I_{34} (three and four aromatic rings)	-0.91
$I_{\geq 5}$ (five and more aromatic rings)	-0.93

Another important parameter characterising the oil type is the American Petroleum Institute gravity, or API gravity. The API gravity is an inverse measure of the relative density of petroleum with respect to water (specific gravity),

$$\text{API gravity} = 141.5/(\text{specific gravity at } 15.6^{\circ}\text{C}) - 131.5\,,$$

but it is used to compare the relative densities of petroleum liquids. If its API gravity is greater than 10, it is lighter and floats on water; if less than 10, it is heavier and sinks. The API gravity is one of the simplest and most wide-spread parameters used for classifying crude oils (Ryder, 2005). The measurements of this parameter for the 8 chosen oil samples demonstrated that it as well exhibits strong correlation with the relative LIF/LIDAR spectrum maximum F_m and thus can be assessed on the basis of *in situ* LIF/LIDAR spectra as well. The value of the corresponding correlation coefficient is 0.73, the data scattering is illustrated in figure 13.

Figure 13: Scattergraphs of the API gravity versus the relative LIF spectrum maximum F_m

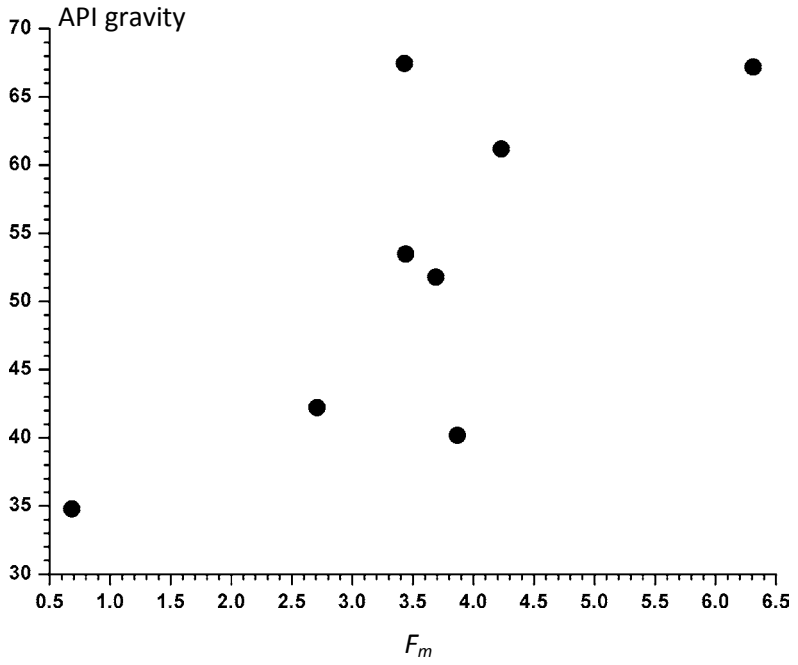

6. FIELD TESTS

The methods developed were field tested in 2009-2011 in the Ria de Vigo and adjacent waters of the Atlantic Ocean with several LIF LIDAR oil detectors installed onboard Coastal Guard vessels (figure 14).

Figure 14: LIF LIDAR oil-spill detectors based on Nd:YAG-3 (a) and XeCl (b) lasers installed onboard of a ship provided by Galician Coastal Guard

Typical 308-nm-excited LIF spectra of predominantly clear waters in different locations of the above mentioned region are shown in figure 15. The curves present an intense and

narrow water Raman peak at 344 nm and a wider peak in the 310-580 nm region due to DOM. The yellow curve corresponds to the only hydrocarbon pollution spot detected and presents specific features: the Raman peak intensity is low due to attenuation by the pollutant, while the pollutant fluorescence adds to the DOM spectrum, leading to a distortion of the broad peak and to a shift of its maximum to about 390 nm.

Figure 15: Typical spectra of unpolluted waters of the Ria of Vigo

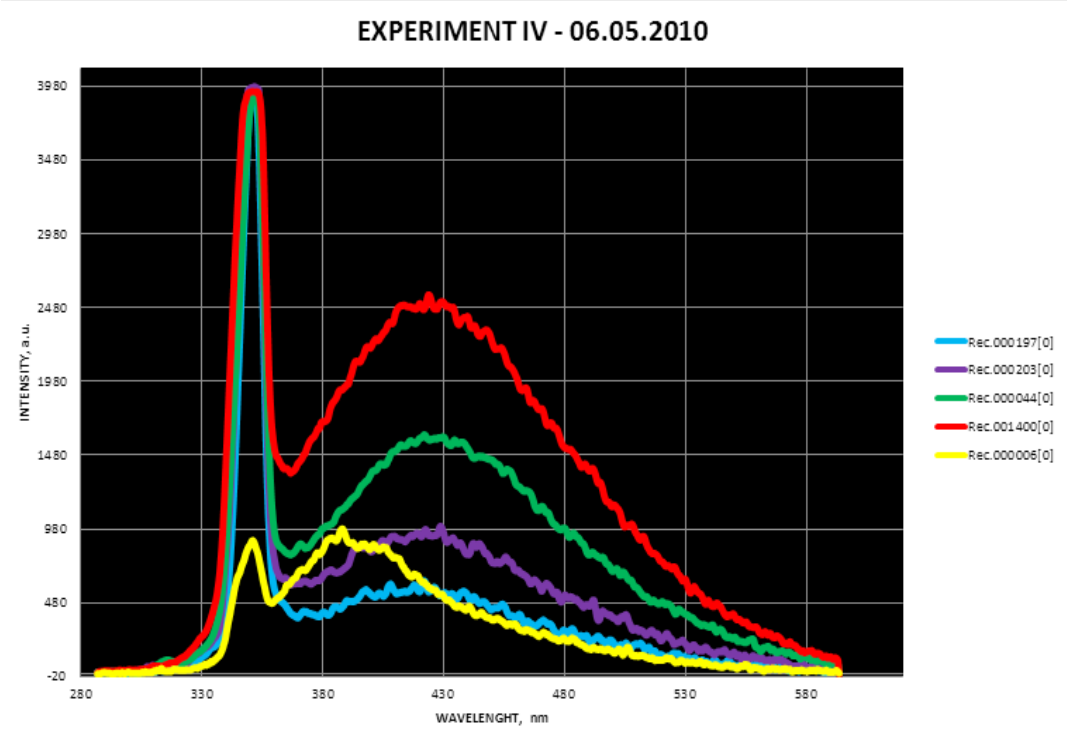

The detector performance for higher pollutant concentrations was tested on controlled experimental spills of rhodamine and fluorescein (figure 16).

Figure 16: Experimental spills of rhodamine and fluorescein

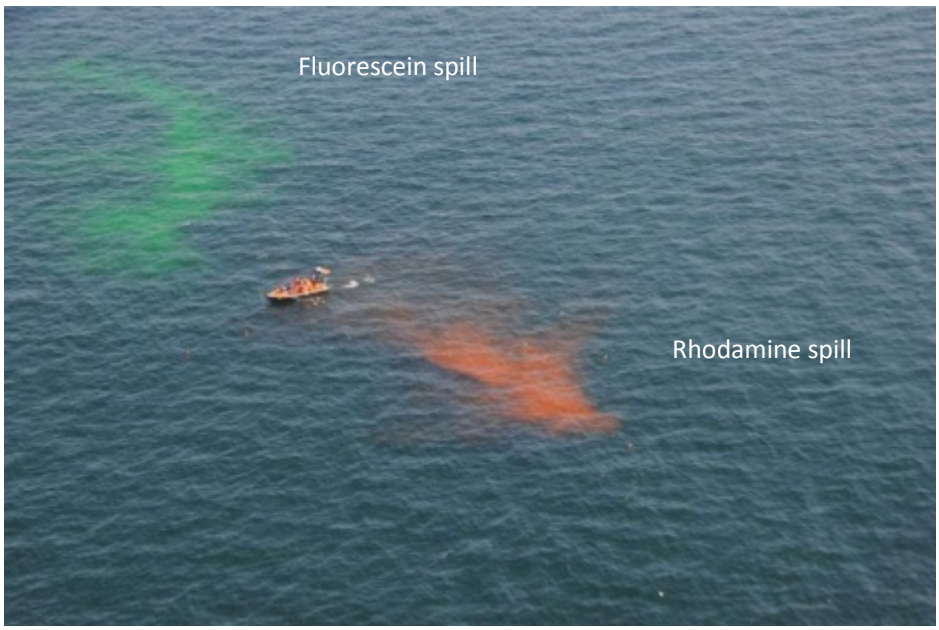

The recorded LIF spectra of waters contaminated by fluorescein are illustrated in figure 17. The spectra differ significantly from those of unpolluted water, with a strong decrease of the relative intensity of Raman peak at 344 nm and of the DOM fluorescence (with a flat maximum at about 430 nm) and present a very strong peak in the green region, which can be ascribed to the fluorescein emission.

Figure 17: Recorded spectra of waters polluted of the Ria of Vigo

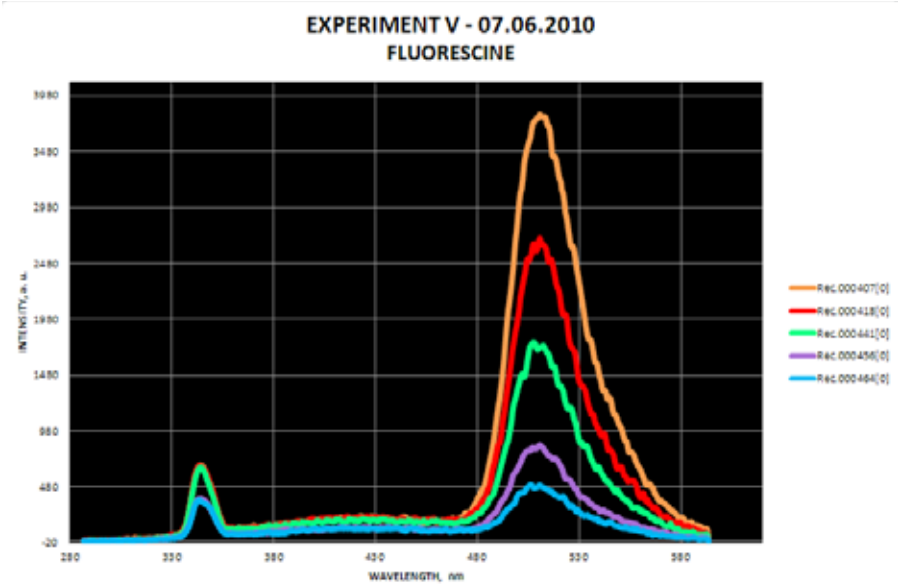

7. CONCLUSION

Investigations carried out within the framework of the DEOSOM project showed great potentiality of the water pollution surveillance and, in particular, the oil spill detection using the analysis of the fluorescence light induced either by a laser (LIF LIDAR technology) or a lamp (SFS technology). It offers high sensitivity, good diagnostic potential, and relatively compact, robust, and simple instrumentation. Wide scalability of the LIF LIDAR technology can be achieved by application of different types of laser and detection units. With the detectors providing the range of more than 100 m, the LIF LIDAR method is suitable not only for the waterborne applications, but for the airborne applications as well.

This opens the prospect of step-by-step deployment of the effective third-level water-pollution surveillance network in the Atlantic-Mediterranean Maritime Cluster, whose elements are adapted to local conditions and scaled in accordance to the assessed accidental pollution risk, providing this way economically feasible and realizable solutions.

The accidents like the Prestige oil tanker disaster have clearly demonstrated especial vulnerability of the bio-environment of the region in question to the oil spills. As such, the prompt and reliable oil-spill monitoring is believed to compose an important part of further developments in the sphere of Sea economic activities. In this connection, it is worthwhile to note that the results of the described research may be applied to other areas of such activities. In particular, Nd:YAG based LIF LIDAR detector was successfully implemented for studying microphytobenthos biomass of muddy and sandy sediments of the Tagus Estuary, Portugal (Vieira et al., 2011) and assessment of water stress in typical plants of Mediterranean coastal zone (Lavrov et al., 2011).

Acknowledgements
This research has been supported in part by Fundação para a Ciência e a Tecnologia (FCT) in Portugal and the European Union within the framework of the European Coordination Action to Foster Prevention and Best Response to Accidental Marine Pollution, Program Accidental Marine Pollution ERA-NET (AMPERA), Project Detection and Evaluation of Oil Spills by Optical Methods (DEOSOM). The authors are grateful to GALP Energia for providing samples of the crudes.

REFERENCES

Alekseyev, V., Babichenko, S. and Sobolev, I. (2008). Control and signal processing system of hyperspectral FLS LiDAR. *2008 International Biennial Baltic Electronics Conference*, 349-352.

AMPERA. (2007). European Coordination Action to Foster Prevention and Best Response to Accidental Marine Pollution, official Web site. Accessed on 14th of August 2011 in: http://www.cid.csic.es/ampera/index.php.

Babichenko, S., Dudelzak, A., Lapimaa, J., Lisin, A., Poryvkina, L. and Vorobiev, A. (2006). Locating water pollution and shore discharges in coastal zone and inland waters with FLS lidar. *EARSeL eProceedings*, **5(1)**: 32–41.

Babichenko, S. and Shchemelyov, S. (2011). Development of compact shipborne LIF LIDAR for oil pollution detection. In: *Book of Abstracts of the International Workshop "Methods for Oil Spill Evaluation", Lisbon, June 29, 2011*, INOV, Lisbon, p. 11. Accessed on 27th of August 2011 in: http://mose.inov.pt/download/abstracts.pdf

Carranza, J.E., Gibb, E., Smith, B.W., Hahn, D.W., and Winefordner, J.D. (2003). Comparison of nonintensified and intensified CCD detectors for laser-induced breakdown spectroscopy, *Applied Optics* **42(30)**: 6016-6021.

Fingas, M. and Brown, C.E. (2007). Oil spill remote sensing: A Forensic approach. In: *Oil Spill Environmental Forensics. Fingerprinting and Source Identification*. Elsevier. Amsterdam.

Hengstermann, T. and Reuter, R. (1992). Laser remote sensing of pollution of the sea: a quantitative approach. *European Association of Remote Sensing Laboratories, Advances in Remote Sensing*, **1(2)**: 52-60.

Lavrov, A., Utkin, A.B., Marques da Silva, J., Vilar, R., Santos, N. M., Alves, B. (2011) Water stress assessment of cork oak leaves and maritime pine needles based on LIF spectra. *Optics and Spectroscopy*, accepted for publication.

Law, R.J. (1980). Analytical methods and their problems in the analysis of oil in water, In: C. S. Johnson and R. J. Morris (eds.), *Oily Water Dicharges – Regulatory, Technical and Scientific Considerations*. Applied Science Publishers. London.

LDI. (2010). *MOD-2LC10212 Multichannel Optical Detector: User Manual*. Laser Diagnostic Instruments Ltd. Tallinn.

Martín, M., Yarovenko, N.V. and Torres, J.M.P. (2011) Oil pollution detection using spectral fluorescent signatures (SFS). In: *Book of Abstracts of the International Workshop "Methods for Oil Spill Evaluation", Lisbon, June 29, 2011*, INOV, Lisbon, p. 13. Accessed on 27th of August 2011 in: http://mose.inov.pt/download/abstracts.pdf

McDougall, A. and McDougall, F.E. (2011). *The Basics of PC Control*. Accessed on 27th of August 2011 in: http://www.pc-control.co.uk/Basics.htm

Ocean Optics. (2011). *HR4000 High-Resolution Spectrometer*. Ocean Optics, Dunedin, FL.

OSPAR. (2006). 1992 OSPAR Convention: Text as amended on 24 July 1998, updated 9 May 2002, 7 February 2005 and 18 May 2006. OSPAR Secretariat. London.

Ryder, A.G. (2005). Analysis of crude petroleum oils using fluorescence spectroscopy. In: C.D. Geddes and J.R. Lakowicz (eds.), *Reviews in Fluorescence 2005*. Springer. New York.

Torres, J.M.P., Yarovenko, N.V. and Martín, J. (2011) LIF/LiDAR techniques for oil spill detection and evaluation. In: *Book of Abstracts of the International Workshop "Methods for Oil Spill Evaluation", Lisbon, June 29, 2011*, INOV, Lisbon, p. 15. Accessed on 27th of August 2011 in: http://mose.inov.pt/download/abstracts.pdf

Utkin, A.B., Lavrov, A. and Vilar, R. (2011). Evaluation of oil spills by laser induced fluorescence spectra. *Proceedings of SPIE*. **7994**: paper 799415.

Vieira, S., Utkin, A.B., Lavrov, A., Santos, N.M., Vilar, R., Marques da Silva, J. and Cartaxana P. (2011). Effects of intertidal microphytobenthos migration on biomass determination via laser-induced fluorescence. *Marine Ecology Progress Series*. **432**: 45-52.